A Variational Approach for Adaptive Underwater Sonar Image Denoising

Deshan Chen, Xiumin Chu, Feng Ma
National Engineering Research Center for Water Transport Safety
Wuhan University of Technology
Wuhan, China
dschen@whut.edu.cn

XuanXuan Teng
School of Electric & Electronic Engineering
Wuhan Polytechnic University
Wuhan, China
tengshelly@gmail.com

***Abstract*—Underwater sonar imaging is a significant means for a variety of maritime work. However, the sonar images are corrupted by signal dependent speckle noise, which restricts the potential practical applications. In this paper, we propose a novel variational approach that addresses the adaptive sonar image denoising problem. To accurately describe the signal dependent characteristic of noise for real sensors, we utilize a generalized noise model, which can be adapted to represent various types of noise. With the generalized noise model, we formulate the denoising problem via a variational approach. Finally, we present a modified primal and dual method to efficiently solve the variational minimization problem. Experimental results on both simulated and real data validate the effectiveness and efficiency of our method.**

Keywords—sonar image; signal dependent noise;speckle noise; image denoising; variational method

I. INTRODUCTION

Sonar images play a significant role in underwater tasks, such as waterway survey, underwater construction inspection, target detection, object recognition, and etc. However, the quality of sonar images is severely degraded by speckle noise, due to the complexity of underwater acoustic propagation as well as the coherent nature of their acquisition processes. Therefore, sonar image denoising, a technique of recovering the underlying clean and sharp image from a noisy observation, is fundamental for its further applications.

In the field of image processing, image denoising has been well studied, and continues to be considerably active [1][2]. However, most state-of-the-art denoising algorithms assume that the observed image is corrupted by signal-independent additive white Gaussian noise [4]-[6], as this makes both analysis and estimation more tractable. However, underwater sonar images are highly affected by signal-dependent multiplicative speckle noise. It is thus that the performance may not be desirable if those methods are directly applied to underwater sonar images.

Speckle noise occurs not only in underwater sonar images, but also in laser images, microscopic images, synthetic aperture radar (SAR) images and medical ultrasonic images. Previous work on multiplicative noise removal generally assumes a specific noise model [7]-[9]. However, due to the complicated imaging conditions, such as the complexity of underwater acoustic channel, the different temperature and salinity of seawater in different locations, underwater sonar images may have different statistical properties and signal dependence under different imaging conditions, where one single noise model may not be able to accurately describe the diverse cases.

As variational approaches for underwater sonar image denoising is not well investigated, in this work, we propose a variational approach to handle the challenging image denoising problem that can be adaptive for complicated real imaging scenario. We adopt a generalized noise model, which can represent various types of noise. Consequently, with the generalized noise model, we formulate the adaptive underwater sonar image denoising as a variational optimization problem, which is, in fact, an optimal estimation from the maximum a posteriori (MAP) point of view. To efficiently solve the variational problem, we present an improved primal-dual algorithm.

The remainder of the paper is organized as follows. Section II proposes the framework of our variational approach based on the generalized noise model and presents an efficient optimization procedure. Experiments on both synthetic and real image data are carried out in section III. Finally, we provide some discussion and conclude the paper in section IV.

II. VARIATIONAL SONAR IMAGE DENOISING

A. Generalized Noise Model

In the previous work, speckle noise is model in several different yet relative ways. Tuthill, T.A et al. argued that the speckle noise followed a Rayleigh distribution and satisfied multiplicative model [10], i.e.,

$$f = un. \tag{1}$$

Where, f is observed noise image, u is underlying noise-free image and n is noise which follows the Rayleigh distribution. The density function is

$$p(x) = \frac{x}{\sigma^2}\exp\left(-\frac{x^2}{2\sigma^2}\right), \tag{2}$$

where $\sigma > 0$ is a parameter. However, it is showed that the speckle noise in the displayed images no longer follows the Rayleigh distribution [11]. In [6], Rudin et al. assumed that the speckle noise model as follows.

$$f = u + un, \tag{3}$$

978-1-5386-0437-3/17/$31.00 ©2017 IEEE

where n the is a zero-mean Gaussian random variable. Relevant to (3), experimental measurements in [12] indicate that the displayed ultrasonic images can be modelled as corrupted with signal-dependent noise of the form:

$$f = u + \sqrt{u}n. \tag{4}$$

In this work, we assume the following generalized signal dependent noise model to deal with mutable signal dependence caused by different imaging conditions in practical applications,

$$f = u + u^{\gamma}n, \tag{5}$$

where n is a Gaussian random variable with zero mean and a standard deviation σ, i.e. $n \sim \mathcal{N}(0, \sigma^2)$, γ is the non-negative exponential parameter which controls the dependence on the signal. It is obvious that model (3) and (4) is a specific case of (5) with γ being 1 and 0.5, respectively.

B. Variational Formulation

With the generalized noise model described in (5), the denoising problem is formulated as follows. Minimizing

$$E = \iint_{\Omega} \frac{\lambda}{2}\left(\frac{f-u}{u^{\gamma}}\right)^2 + |\nabla u| dxdy \tag{6}$$

over some domain of interest Ω in the image plane, where λ is a parameter, $|\nabla u| = \sqrt{\left(\frac{\partial u}{\partial x}\right)^2 + \left(\frac{\partial u}{\partial y}\right)^2}$.

The formulation can be explained as follows. The first term in (6), named the fidelity term, is to guarantee that the recovered image is consistent with the noise observation according to (5). The second term is total variation (TV), a regularizer used to penalize the roughness of the solution. A TV model preserves edges well while removing noise effects and has proven to be an effective method applicable to a range of problems in image processing and computer vision, such as reconstruction, denoising, and deblurring. λ is a positive scalar factor that weighs the relative contributions of these two terms. Note that λ depends upon the noise level of the observed noise image; the noisier the image, the smaller should the value of λ be. This is apparent based on a statistical interpretation as follows.

We may formulate (6) into a maximum a posteriori (MAP) problem.

$$u = \underset{u}{\operatorname{argmax}}\, \mathcal{P}(u|f). \tag{7}$$

Bayesian formula indicates that

$$\mathcal{P}(u|f) \propto \mathcal{P}(f|u)\mathcal{P}(u), \tag{8}$$

where $\mathcal{P}(f|u)$ and $\mathcal{P}(u)$ denote the likelihood and prior distribution, respectively, as follows.

$$\mathcal{P}(f|u) \propto \prod_{(x,y)\in\Omega} \exp\left(-\frac{(f-u)^2/u^{2\gamma}}{2\sigma^2}\right)$$

$$\mathcal{P}(u) \propto \prod_{(x,y)\in\Omega} \exp\left(-\frac{|\nabla u|}{b}\right) \tag{9}$$

(10)

where b is the variance of the Laplacian prior on ∇u and σ^2 is the variance of the noise. Taking the negative log likelihood to the posteriori in (8) leads to

$$-\log \mathcal{P}(u|f) = \iint_{\Omega} \frac{1}{2\sigma^2}\left(\frac{f-u}{u^{\gamma}}\right)^2 dxdy + \iint_{\Omega} \frac{|\nabla u|}{b} dxdy + \text{Constant} \tag{11}$$

We can thus observe that MAP (7) leads to the exact optimization problem in (6), with $\lambda = \frac{b}{\sigma^2}$, and the fidelity term and TV regularizer correspond to the likelihood and prior distribution, respectively. Suppose the Laplacian variance b is fixed, the noisier the data (σ^2 is large), the smaller the value of λ should be.

C. Numerical Solution

The most straightforward idea to optimize (6) is to apply gradient decent algorithm with the following corresponding Euler-Lagrange equation,

$$\lambda\left(\frac{(u-f)[(1-\gamma)u+\gamma f]}{u^{2\gamma+1}}\right) - div\left(\frac{\nabla u}{|\nabla u|}\right) = 0. \tag{12}$$

Despite of its simplicity, the method is generally slow, due to the low convergence rate. Motivated by the primal-dual method proposed in [14], a considerably efficient algorithm for TV minimization problems, we adapt the idea into our scenario. To this end, we can formulate the TV norm into its dual form through introducing the corresponding dual variable, shown as follows,

$$|\nabla u| = \sup\{p \cdot \nabla u : \|p\| < 1\} \tag{13}$$

where $p \in \mathbb{R}^2$ is the dual variable. Consequently, we obtain the saddle point problem of the minimization problem (6),

$$\min_{u} \max_{\|p\|<1} \iint_{\Omega} \frac{\lambda}{2}\left(\frac{f-u}{u^{\gamma}}\right)^2 + (p \cdot \nabla u) dxdy \tag{14}$$

To solve (14), we adopt the primal-dual scheme that performs commutatively between the following two steps:

(a) Projected gradient ascent in the dual variable:

$$p^{k+1} = \frac{p^k + \delta \nabla u^k}{\max\{|p^k + \delta \nabla u^k|, 1\}} \tag{15}$$

(b) Semi-implicit gradient descent step in the primal variable:

$$u^{k+1} = u^k - \tau(\lambda \omega(u^k)(u^{k+1} - f) - div\, p^{k+1}), \tag{16}$$

where $\omega(u^k) = \frac{(1-\gamma)u^k + \gamma f}{u^{k\,2\gamma+1}}$. We can deduce the following iterative scheme,

$$u^{k+1} = \frac{u^k + \tau\lambda f + \tau div\, p^{k+1}}{1 + \tau\omega(u^k)} \tag{17}$$

978-1-5386-0437-3/17/$31.00 ©2017 IEEE

where δ, τ are positive constants denoting step size, k denotes the iteratiion index.

The numerical method is summarized in Algorithm 1 as follows.

Algorithm I.

1: Initialization: $u^0 = f, p = \mathbf{0}$, fixed δ, τ
2: Estimate parameter γ via the method proposed in [15]
3: While not converged, do
4: Update dual variable with (15);
5: Update primal variable with (17);
6: Output u

III. Experiment Results

In this section, we present experimental results for our proposed models. To vividly reveal the efficiency and effectiveness of our method, we test using both simulation data and real underwater sonar images. All experiments were implemented using MATLAB R2015b on a desktop PC with an Intel CPU at 2.0GHz, 8GB RAM, and a 64-bit Window 10 operating system.

We utilize the relative error and maximum iteration number as the stop criterion for our method given by

$$\frac{\|u^{k+1} - u^k\|}{\|u^k\|} < 10^{-4} \; or \; k > M$$

where M = 200 is the maximum iteration number. We experientially set $\delta = 0.25, \tau = 1.0$ for our primal-dual scheme in Algorithm I.

A. Simulated results

In the experiments, all test images have intensity values in the range of [0, 255]. In this numerical test, we used a synthetic image, as shown in Fig. 1. The test image was corrupted using (5) as the degradation model, with γ = 0.8 and 1.5, σ = 2 and 4.

In order to measure the quality of the restored images, we compute the peak signal-to noise ratio (PSNR) value and the structure similarity (SSIM) index defined as follows:

$$\mathrm{PSNR}(u^*, \bar{u}) = 10 \log_{10}\left(\frac{255^2 mn}{\|u^* - \bar{u}\|^2}\right) \tag{18}$$

$$\mathrm{SSIM}(u^*, \bar{u}) = \frac{(2\mu_{\bar{u}}\mu_{u^*} + c_1)(\sigma_{u^*\bar{u}} + c_2)}{\left(\mu_{\bar{u}}{}^2 + \mu_{u^*}{}^2 + c_1\right)\left(\sigma_{\bar{u}}{}^2 + \sigma_{u^*}{}^2 + c_2\right)} \tag{19}$$

where $u^* \in \mathbb{R}^{m\times n}$ is the clean image, $\bar{u} \in \mathbb{R}^{m\times n}$is the restored image, μ_u is the average of u, σ_u is the standard deviation of u, and c_1 and c_2 are some constants for stability.

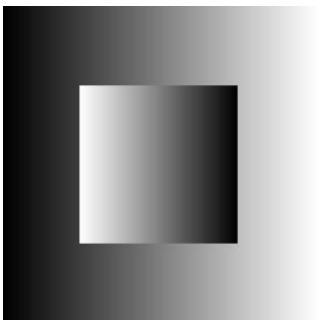

Fig.1 Synthetic test image for simulated evaluation.

TABLE I. Comparison results for PSNR and SSIM

Noise Level		Fixed γ = 0.5		Fixed γ = 1		Correct γ	
Fig.1	σ	PSNR	SSIM	PSNR	SSIM	PSNR	SSIM
γ = 0.4	1	42.03	0.9869	34.05	0.9702	**44.56**	**0.9874**
	2	38.52	0.9807	32.72	0.9616	**39.97**	**0.9818**
γ = 0.8	1	18.35	0.7021	25.41	0.9660	**26.08**	**0.9704**
	2	17.02	0.8976	19.69	0.9268	**20.06**	**0.9328**
γ = 1.2	1	11.44	0.8748	13.95	0.8819	**13.95**	**0.8832**
	2	**12.91**	0.8266	12.82	0.8341	12.82	**0.8348**

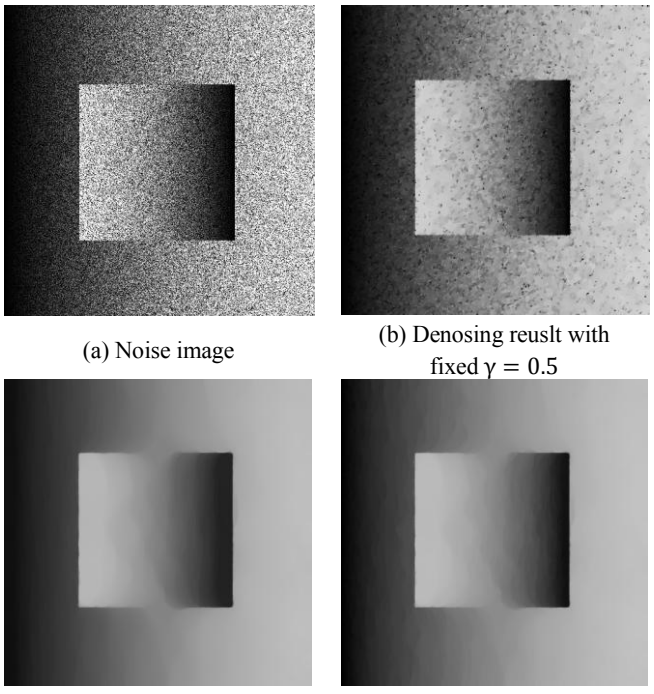

(a) Noise image (b) Denosing reuslt with fixed γ = 0.5

(c) Denosing reuslt with fixed γ = 1.0 (d) Denosing reuslt with correct γ = 0.8

Fig.2 Simulated denoising results for the case of γ = 0.8, σ = 2 .

978-1-5386-0437-3/17/$31.00 ©2017 IEEE

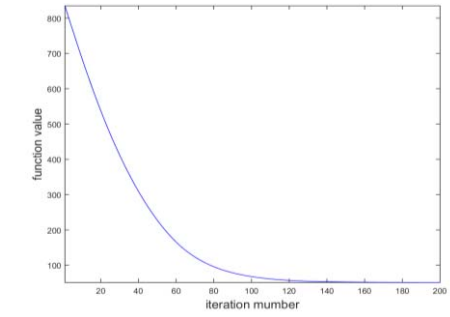

(a) function value

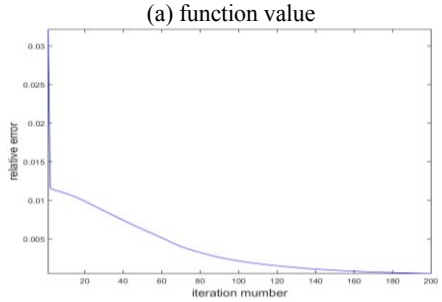

(b) relative error

Fig. 3 Objective function value and relative error of the proposed method.

In Fig.2, we display the denoised images with different parameter γ, for the specific case with $\gamma = 0.8, \sigma = 2$. As visually displayed, our method could performance well once the parameter γ is properly associated. To analyze the influence of the parameter γ, we conduct extensive experiments on a combination of noise level and evaluate the corresponding denoising performance. As shown in Table I, our method could achieve high SSIM even when the noise level is considerably high, when γ is correctly associated. As we can also observe that the PSNR value tends to decrease dramatically, which seems that it is not consistent with SSIM. We consider this is due to the fact that the added artificial noise varies the average intensity of the image, while the proposed method preserves the average intensity otherwise. This causes a different image contrast with original image, leading and in turn resulting in a low PSRN.

Moreover, we can observe from Fig.2 (b) that too small parameter γ causes insufficient denoising, where a large amount of noise remains. In contrast, too large parameter γ cause over-smoothing. However, as mentioned previously, the TV model has a good property that it preserves edge well, which relieves the blurring effect caused by large γ.

Fig. 3 shows the function values and relative errors during the maximum iterations for the case of the 'Synthetic' image corrupted with$\gamma = 0.8, \sigma = 2$. We can observe that the function value is monotonically decreasing, which indicate stable iterations. Both the function value and relative error decrease very fast, implying the efficiency of our numerical method.

B. Real-image results

In this subsection, we apply the proposed method to side scan sonar (SSS) image and synthetic aperture sonar (SAS) image, separately. We estimate the signal dependence parameter γ from the observed noise image via the method proposed in [15].

(a) observed noise image (b) denoised image

Fig. 4 Denoising result on a real SSS image.

Fig. 4 shows a denoising result on a real SSS image, where the estimated parameter $\gamma = 0.5314$. As shown in the denoised image, the "chain" part in the image tends to be more recognizable, while the details on the background seabed are still preserved well.

Fig. 5 shows another denoising result on a real SAS image. Compared with SSS image, SAS image generally has higher resolution and less noise level. The estimated parameter $\gamma = 1.217$. Compared with the SSS image in Fig.3, this image has a stronger signal-dependence. As the proposed method is adaptive to such signal-dependence, the denoised image displays that the noise in the background region is filtered out sufficiently, while the foreground objects and shadow regions are still considerably distinct.

(a) observed noise image

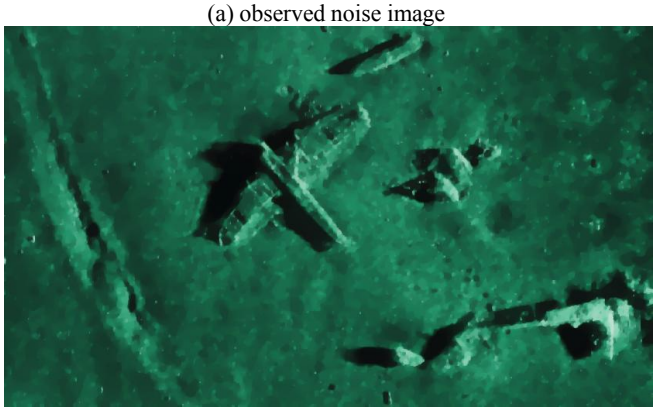

(b) denoised image

Fig. 5 Denoising result on a real SAS image.

978-1-5386-0437-3/17/$31.00 ©2017 IEEE

IV. Conclusion and Disscusion

In this paper, we have proposed a variational approach for recovering the underlying noise-free image from an underwater noisy observation. The variational minimization problem is constructed base on a generalized noise model, which could be applicable to varying signal-dependence of noise due to practically complicated imaging conditions. To effectively solve the variational problem, we adapt the primal-dual algorithm into our case. Extensive simulation experiments indicate that too large or too small a signal-dependence parameter may lead to over-smoothing or leaving unfiltered noise. Based on the estimation of signal-dependence parameter from the observed noise image, we can conduct adaptive denoising for real underwater sonar images.

For future work, the proposed method could be extended in some directions as well. First, incorrect estimated parameter may deduce undesirable results as the parameter estimation procedure is absolutely independent with denoising progress. The investigation on the cooperation between the two schemes is of interest, which may produce more reliable results. Moreover, using dictionary learning based sparseness prior rather than TV prior [16] is also interesting and worthy of investigation.

Acknowledgment

This work was supported by NSFC (51609193). The authors would like to thank the reviewers for their helpful comments.

References

[1] P. Chatterjee and P. Milanfar, Fundamental Limits of Image Denoising: Are We There Yet?, Proc. of IEEE Intl. Conf. on Acoustics, Speech and Signal Processing (ICASSP), Dallas, TX, March 2010.

[2] P. Chatterjee and P. Milanfar, Is Denoising Dead?, IEEE Transactions on Image Processing, vol. 19, num. 4, pp 895-911, Apr. 2010.

[3] Dabov K, Foi A, Katkovnik V, et al. Image denoising by sparse 3-D transform-domain collaborative filtering. IEEE Transactions on Image Processing, 2007, 16(8):2080-2095.

[4] Portilla J, Strela V, Wainwright M J, et al. Image denoising using scale mixtures of Gaussians in the wavelet domain. IEEE Transactions on Image Processing, 2003, 12(11):1338-1351.

[5] Chatterjee P, Milanfar P. Clustering-based denoising with locally learned dictionaries. IEEE Transactions on Image Processing, 2009, 18(7):1438-1451.

[6] L. Rudin, P.-L. Lions, S. Osher, Multiplicative Denoising and Deblurring: Theory and Algorithms, in Geometric Level Set Methods in Imaging Vision, and Graphics, Springer, New York, 2003. pp. 103–119.

[7] Krissian K, Kikinis R, Westin C F, et al. Speckle-Constrained Filtering of Ultrasound Images. IEEE Computer Society Conference on Computer Vision and Pattern Recognition. IEEE Computer Society, 2005:547-552.

[8] Liu M, Fan Q. A modified convex variational model for multiplicative noise removal. Journal of Visual Communication & Image Representation, 2016, 36:187-198.

[9] Jin Z, Yang X. A Variational Model to Remove the Multiplicative Noise in Ultrasound Images. Journal of Mathematical Imaging and Vision, 2011, 39(1):62-74.

[10] Tuthill, T.A., Sperry, R.H., Parker, K.J.: Deviation from Rayleigh statistics in ultrasonic speckle. Ultrason. Imag. 10, 81–90 (1988).

[11] Loupas, A.: Digital image processing for noise reduction in medical ultrasonics. PhD thesis, University of Edinburgh, UK (1988).

[12] Brezis, H.: Operateures Maximaux Monotone. North-Holland, Amsterdam (1993).

[13] Liu X, Tanaka M, Okutomi M. Signal dependent noise removal from a single image. IEEE International Conference on Image Processing. IEEE, 2015:2679-2683.

[14] A. Chambolle, T. Pock: A first-order primal-dual algorithm for convex problems with applications to imaging, Journal of Mathematical Imaging and Vision 40(1):120-145, 2011.

[15] Liu, Xinhao, M. Tanaka, and M. Okutomi. "Estimation of signal dependent noise parameters from a single image." IEEE International Conference on Image Processing IEEE, 2013:79-82.

[16] Wright, John, et al. "Sparse Representation for Computer Vision and Pattern Recognition." Proceedings of the IEEE 98.6(2010):1031-1044.

978-1-5386-0437-3/17/$31.00 ©2017 IEEE